

# Full depth CNN classifier for handwritten and license plate characters recognition

Mohammed Salemdeeb<sup>Corresp., 1</sup>, Sarp Ertürk<sup>2</sup>

<sup>1</sup> Dep. of Electrical-Electronics Engineering, Bartin University, Bartin, Turkey

<sup>2</sup> Dep. of Electronics & Communication Eng., Kocaeli University, Izmit, Kocaeli, Turkey

Corresponding Author: Mohammed Salemdeeb  
Email address: msalemdeeb@bartin.edu.tr

Character recognition is an important research field of interest for many applications. In recent years, deep learning has made breakthroughs in image classification, especially for character recognition. However, convolutional neural networks (CNN) still deliver state-of-the-art results in this area. Motivated by the success of CNNs, this paper proposes a simple novel full depth stacked CNN architecture for Latin and Arabic handwritten alphanumeric characters that is also utilized for license plate (LP) characters recognition. The proposed architecture is constructed by four convolutional layers, two max-pooling layers, and one fully connected layer. This architecture is low-complex, fast, reliable and achieves very promising classification accuracy that may move the field forward in terms of low complexity, high accuracy and full feature extraction. The proposed approach is tested on four benchmarks for handwritten character datasets, Fashion-MNIST dataset, public LP character datasets and a newly introduced real LP isolated character dataset. The proposed approach tests report an error of only 0.28% for MNIST, 0.34% for MAHDB, 1.45% for AHCD, 3.81% for AIA9K, 5.00% for Fashion-MNIST, 0.26% for Saudi license plate character and 0.97% for Latin license plate characters datasets. The license plate characters include license plates from Turkey (TR), Europe (EU), USA, United Arab Emirates (UAE) and Kingdom of Saudi Arabia (KSA).

# 1 Full Depth CNN Classifier for Handwritten 2 and License Plate Characters Recognition

3 Mohammed Salemdeeb<sup>1</sup> and Sarp Ertürk<sup>2</sup>

4 <sup>1</sup>Dep. of Electrical-Electronics Engineering, Bartin University, Bartin, Turkey.

5 <sup>2</sup>Dep. of Electronics & Communication Eng., Kocaeli University, Izmit, Kocaeli, Turkey

6 Corresponding author:

7 Mohammed Salemdeeb<sup>1</sup>

8 Email address: msalemdeeb@bartin.edu.tr

## 9 ABSTRACT

10 Character recognition is an important research field of interest for many applications. In recent years,  
11 deep learning has made breakthroughs in image classification, especially for character recognition.  
12 However, convolutional neural networks (CNN) still deliver state-of-the-art results in this area. Motivated  
13 by the success of CNNs, this paper proposes a simple novel full depth stacked CNN architecture for Latin  
14 and Arabic handwritten alphanumeric characters that is also utilized for license plate (LP) characters  
15 recognition. The proposed architecture is constructed by four convolutional layers, two max-pooling layers,  
16 and one fully connected layer. This architecture is low-complex, fast, reliable and achieves very promising  
17 classification accuracy that may move the field forward in terms of low complexity, high accuracy and  
18 full feature extraction. The proposed approach is tested on four benchmarks for handwritten character  
19 datasets, Fashion-MNIST dataset, public LP character datasets and a newly introduced real LP isolated  
20 character dataset. The proposed approach tests report an error of only 0.28% for MNIST, 0.34% for  
21 MAHDB, 1.45% for AHCD, 3.81% for AIA9K, 5.00% for Fashion-MNIST, 0.26% for Saudi license plate  
22 character and 0.97% for Latin license plate character datasets. The license plate characters include  
23 license plates from Turkey (TR), Europe (EU), USA, United Arab Emirates (UAE) and Kingdom of Saudi  
24 Arabia (KSA).

## 25 INTRODUCTION

26 Character recognition (CR) plays a key role in many applications and motivates R&D in the field for  
27 accurate and fast classification solutions. CR has been widely investigated in many languages using  
28 different proposed methods. In the last years, researchers widely used CNN as deep learning classifiers and  
29 achieved good results on handwritten Alphanumeric in many languages (Lecun et al., 1998; Abdleazeem  
30 and El-Sherif, 2008; El-Sawy et al., 2017; Guha et al., 2020), character recognition in real-world images  
31 (Netzer et al., 2011), document scanning, optical character recognition (OCR) and automatic license  
32 plate character recognition (ALPR) (Comelli et al., 1995). Searching for text information in images is a  
33 time-consuming process that largely benefits of CR. Particularly, in Arabic language the connectivity of  
34 letters make a challenge for classification (Eltay et al., 2020). Therefore, isolated character datasets get  
35 more interest in research.

36 MNIST is a handwritten digits dataset introduced by Lecun et al. (1998) and used to test supervised  
37 machine learning algorithms. The best accuracy obtained by stacked CNN architectures, until before  
38 two years, is a test error rate of 0.35% in (Cireşan et al., 2010), where large deep CNN of nine layers  
39 with an elastic distortion applied to the input images. Narrowing the gap to human performance, a new  
40 architecture of five committees of seven deep CNNs with six width normalization and elastic distortion  
41 was trained and tested in (Ciresan et al., 2011) and reported an error rate of 0.27%, where the main CNN  
42 is seven stacked layers. In (Ciregan et al., 2012), a near-human performance error rate of 0.23% was  
43 achieved, where several techniques were combined in a novel way to build a multi-column deep neural  
44 network (MCDNN) inspired by micro-columns of neurons in cerebral cortex compared to the number of  
45 layers found between retina and visual cortex of macaque monkeys.

46 Recently, Moradi et al. (2019) developed a new CNN architecture with orthogonal feature maps based

47 on Residual modules of ResNet (He et al., 2016) and Inception modules of GoogleNet (Szegedy et al.,  
48 2015), with 534474 learnable parameters which are equal to SqueezeNet (Iandola et al., 2016) learnable  
49 parameters, and thus the model reported an error of 0.28%. However, a CNN architecture for small  
50 size input images of  $20 \times 20$  pixels was proposed in (Le and Nguyen, 2019). In addition, a multimodal  
51 deep learning architecture was proposed in (Kowsari et al., 2018), where deep neural networks (DNN),  
52 CNN and recurrent neural networks (RNN) were used in one architecture design achieving an error of  
53 0.18%. A plain CNN with stochastic optimization method was proposed in (Assiri, 2019), this method  
54 applied regular Dropout layers after each pooling and fully connected (FC) layers, this 15 stacked layers  
55 approach obtained an error of 0.17% by 13.21M parameters. Hirata and Takahashi (2020) proposed an  
56 architecture with one base CNN and multiple FC sub-networks, this 28 spars layers architecture with  
57 28.67M parameters obtained an error of 0.16%. Byerly et al. (2020) presented a CNN design with  
58 additional branches after certain convolutions, and from each branch, they transformed each of the final  
59 filters into a pair of homogeneous vector capsules, this 21 spars layers obtained an error of 0.16%.

60 While MNIST was well studied in the literature, there were only a few works on Arabic handwritten  
61 character recognition (Abdleazeem and El-Sherif, 2008). The large Arabic Handwritten Digits (AHDBase)  
62 has been introduced in (El-Sherif and Abdelazeem, 2007). Abdleazeem and El-Sherif (2008) modified  
63 AHDBase to be MADBase and evaluated 54 different classifier/features combinations and reported a  
64 classification error of 0.52% utilizing radial basis function (RBF) and support vector machine (SVM).  
65 Also, they discussed the problem of Arabic zero, which is just a dot and smaller than other digits. They  
66 solved the problem by introducing a size-sensitive feature which is the ratio of the digit bounding box area  
67 to the average bounding box area of all digits in AHDBase's training set. In the same context, Mudhsh and  
68 Almodfer (2017) obtained a validation error of 0.34% on the MADBase dataset by using an Alphanumeric  
69 VGG network inspired by the VGGNet (Simonyan and Zisserman, 2015) with dropout regularization and  
70 data augmentation but the error performance does not hold on the test set.

71 Toriki et al. (2014) introduced AIA9K dataset and reported a classification error of 5.72% on the  
72 test set by using window-based descriptors with some common classifiers such as logistic regression,  
73 linear SVM, nonlinear SVM and artificial neural networks (ANN) classifiers. Younis (2017) tested a  
74 CNN architecture and obtained an error of 5.2%, he proposed a stacked CNN of three convolution layers  
75 followed by batch normalization, rectified linear units (ReLU) activation, dropout and two FC layers.

76 The AHCD dataset was introduced by El-Sawy et al. (2017), they reported a classification error of  
77 5.1% using a stacked CNN of two convolution layers, two pooling layers and two FC layers. Najadat  
78 et al. (2019) obtained a classification error of 2.8% by using a series CNN of four convolution layers  
79 activated by ReLU, two pooling layers and three FC layers. The state-of-the-art result for this dataset  
80 is a classification error of 1.58% obtained by Sousa (2018), it was achieved by ensemble averaging of  
81 four CNNs, two inspired by VGG16 and two written from scratch, with batch normalization and dropout  
82 regularization, to form 12 layers architecture called VGG12.

83 For benchmarking machine learning algorithms on tiny grayscale images other than Alphanumeric  
84 characters, Xiao et al. (2017) introduced Fashion-MNIST dataset to serve as a direct replacement for  
85 the original MNIST dataset and reported a classification test error of 10.3% using SVM. This dataset  
86 gained the attention of many researchers to test their approaches and better error of 3.65% was achieved  
87 by Zhong et al. (2017) in which a random erasing augmentation was used with wide residual networks  
88 (WRN) (Zagoruyko and Komodakis, 2016). The state-of-the-art performance for Fashion-MNIST is  
89 an error of 2.34% reported in (Zeng et al., 2018) using a deep collaborative weight-based classification  
90 method based on VGG16. Recently, a modelling and optimization based method was used (Chou et al.,  
91 2019) to optimize the parameters for a multi-layer (16 layer) CNN reporting an error of 8.32% and 0.57%  
92 for Fashion-MNIST and MNIST respectively.

93 ALPR is a group of techniques that use CR modules to recognize vehicle's LP number. Sometimes,  
94 it is also referred to as license plate detection and recognition (LPDR). ALPR is used in many real-life  
95 applications (Du et al., 2013) like electronic toll collection, traffic control, security, etc. The main  
96 challenges of detection and recognition of license plates are the variations in the plate types, environments,  
97 languages and fonts. Both CNN and traditional approaches are used to solve vehicle license plates  
98 recognition problems. Traditional approaches involve computer vision, image processing and pattern  
99 recognition algorithms for features such as color, edge and morphology (Xie et al., 2018). A typical ALPR  
100 system consists of three modules, plate detection, character segmentation and CR modules (Shyang-Lih  
101 Chang et al., 2004). This research focuses on CR techniques and compared them with the proposed CR

102 approach. CR modules need an off-line training phase to train a classifier on each isolated character using  
103 a set of manually cropped character images (Bulan et al., 2017). Excessive operational time, cost and  
104 efforts must be considered when manual cropping of character images are needed to be collected and  
105 labeled for training and testing, and to overcome this, artificially generated synthetic license plates were  
106 proposed (Bulan et al., 2015).

107 Additionally, very little research was done on multi-language LP character recognition, the reason  
108 is mostly due to the lack of multi-language LP datasets. Some recent researches were interested in  
109 introducing a global ALPR system. Asif et al. (2017) studied only LP detection module using a histogram-  
110 based approach, and a private dataset was used, which comprised of LPs from Hungary, America, Serbia,  
111 Pakistan, Italy, China, and UAE (Asif et al., 2017). VGG and LSTM were proposed for CR module  
112 in (Dorbe et al., 2018) and the measured CR module accuracy was 96.7% where the test was done on  
113 LPs from Russia, Poland, Latvia, Belarus, Estonia, Germany, Lithuania, Finland and Sweden. Also, tiny  
114 YOLOv3 was used as a unified CR module for LPs from Greece, USA, Croatia, Taiwan, and South Korea  
115 (Henry et al., 2020). Furthermore, several proposed methods interested in multi-language LPCR testing  
116 CR modules on each LP country's dataset separately, without accumulating the characters into one dataset  
117 (Li et al., 2019; Yépez et al., 2019; Asif et al., 2019). In addition, Selmi et al. (2020) proposed a mask  
118 R-CNN detector for character segmentation and recognition concerning Arabic and English LP characters  
119 from Tunisia and USA. Park et al. (2019) concerned USA and Korean LPs describing the problem as  
120 multi-style detection. CNN shrinkage-based architecture was studied in (Salemdeeb and Erturk, 2020),  
121 utilizing the maximum number of convolutional layers that can be added. Salemdeeb and Erturk (2020)  
122 studied the LP detection and country classification problem for multinational and multi-language LPs  
123 from Turkey, Europe, USA, UAE and KSA, without studying CR problem. These researches studied LPs  
124 from 23 different countries where most of them use Latin characters to write the LP number, and totally  
125 five languages were concerned (English, Taiwanese, Korean, Chinese and Arabic). In Taiwan, Korea,  
126 China, UAE, Tunisia and KSA, the LP number is written using Latin characters, but the city information  
127 is coded using characters from that the country's language.

128 In this paper, Arabic and Latin isolated characters are targeted to be recognized using a proposed full  
129 depth CNN (FDCNN) architecture in which the regions of interest are USA, EU and Middle East. To  
130 verify the performance of the proposed FDCNN, some isolated handwritten Arabic and Latin characters  
131 benchmarks such as MNIST, MADbase, AHCD, AIA9K datasets are also tested. Also, a new dataset  
132 named LP Arabic and Latin isolated characters (LPALIC) is introduced and tested. In addition, the recent  
133 FashionMNIST dataset is also tested to generalize the full depth feature extraction approach performance  
134 on tiny grayscale images. The proposed FDCNN approach closes the gap between software and hardware  
135 implementation since it provides low complexity and high performance. All the trained models and the  
136 LPALIC dataset<sup>1</sup> are made publicly available online for research community and future tests.

137 The rest of this paper is organized as follows; section 2 introduces the structure of datasets used in  
138 this paper and also the new LPALIC dataset. In section 3, the proposed approach is described in details.  
139 Section 4 presents a series of experimental results and discussions. Finally, section 5 summarizes the  
140 main points of the entire work as a conclusion.

## 141 DATASETS

### 142 Datasets Available in the Literature

143 MNIST is a low-complexity data collection of handwritten digits to test supervised machine learning  
144 algorithms introduced by Lecun et al. (1998). It has grayscale images of size  $28 \times 28$  pixels with 60000  
145 training digits and 10000 test digits written by different persons. The digits are white and have black  
146 background, normalized to  $20 \times 20$  pixels preserving the aspect ratio, and then centered at the center of  
147 mass of the  $28 \times 28$  pixels grayscale images. The official site for the dataset and results are available by  
148 LeCun<sup>2</sup>.

149 In MADbase, 700 Arabic native writers wrote ten digits ten times and the images were collected as  
150 70000 binary images; 60000 for training and 10000 for testing, so that writers of training set and test set  
151 are exclusive. This dataset<sup>3</sup> has the same format as MNIST to make veracity for comparisons between

<sup>1</sup><https://www.kaggle.com/dataset/b4697afbddab933081344d1bed3f7907f0b2b2522f637adf15a5fcea67af2145>

<sup>2</sup><http://yann.lecun.com/exdb/mnist/>

<sup>3</sup><http://datacenter.aucegypt.edu/shazeem>

152 digits (used in Arabic and English languages) recognition approaches. Table 1 shows example digits  
 153 of printed Latin, Arabic and handwritten Arabic characters used for numbers as declared in ISO/IEC  
 8859-6:1999.

**Table 1.** Printed and handwritten digits.

Printed Latin Characters	0	1	2	3	4	5	6	7	8	9
Printed Arabic Characters	٠	١	٢	٣	٤	٥	٦	٧	٨	٩
Handwritten	٠	١	٢	٣	٤	٥	٦	٧	٨	٩

154

155 AHCD dataset<sup>4</sup> consists of 13440 training images and 3360 test images for 28 Arabic handwritten  
 156 letters (classes) of size  $32 \times 32$  pixels grayscale images. In AI9IK<sup>5</sup> dataset, 62 female and 45 male Arabic  
 157 native writers aged between 18 to 25 years old at the Faculty of Engineering at Alexandria University-  
 158 Egypt were invited to write all the Arabic letters 3 times to gather 8988 letters of which 8737  $32 \times 32$   
 159 grayscale letter images were accepted after a verification process by eliminating cropping errors, writer  
 160 mistakes and unclear letters. FashionMNIST dataset<sup>6</sup> has images of 70000 unique products taken by  
 161 professional photographers. The thumbnails ( $51 \times 73$ ) were then converted to  $28 \times 28$  grayscale images  
 162 by the conversion pipeline declared in (Xiao et al., 2017). It is composed of 60000 training images and  
 163 10000 test images of 10 class labels.

164

Table 2 gives a brief review on some publicly available related LP datasets for LPDR problem. The  
 Zemris dataset is also called English LP in some references (Panahi and Gholampour, 2017).

**Table 2.** A review of publicly available ALPR datasets.

Dataset	Approach	Number of Images	Accuracy	Classifier	Character Set	Purpose
Zemris	Kraupner (2003)	510	86.2%	SVM	No	LPDR
UCSD	Dlagnekov (2005)	405	89.5%	OCR	No	LPDR
Snapshots	Martinsky (2007)	97	85%	MLP	No	LPDR
ARG	Fernández et al. (2011)	730	95.8%	SVM	No	LPDR
SSIG	Gonçalves et al. (2016)	2000	95.8%	SVM-OCR	Yes	LPDR
ReId	Špaňhel et al. (2017)	77k	96.5%	CNN	No	LPR
UFPR	Laroca et al. (2018)	4500	78.33%	CR-NET	Yes	LPDR
CCPD	Xu et al. (2018)	250k	95.2%	RPnet	Yes	LPDR

165

### 166 Novel License Plate Characters Dataset

167

This research introduces a new multi-language LP characters dataset, involving both Latin and Arabic  
 168 characters from LP images used in Turkey, USA, UAE, KSA and EU (Croatia, Greece, Czech, France,  
 169 Germany, Serbia, Netherlands and Belgium ). It is called LPALIC dataset. In addition, some characters  
 170 cropped from Brazil, India and other countries were added for just training to give features diversity.  
 171 Furthermore, Some characters were collected from some public LP datasets, LP websites and our own  
 172 camera pictures in Turkey taken in different weather conditions, places, blurring, distances, tilts and  
 173 illuminations. These characters are real LP manually cropped characters without any filtering. For  
 174 uniformity a size of  $28 \times 28$  pixels of grayscale images was utilized.

175

The manually cropped characters were fed into the following conversion pipeline inspired from  
 176 FashionMNIST (Xiao et al., 2017) which is similar to MNIST (Lecun et al., 1998) ,

177

1. Resizing the longest edge of the image to 24 to save the aspect ratio.

178

2. Converting the image to 8-bit grayscale pixels image.

<sup>4</sup><https://www.kaggle.com/mloey1/ahcd1>

<sup>5</sup>[www.eng.alexu.edu.eg/%7Emehussein/AIA9k/index.html](http://www.eng.alexu.edu.eg/%7Emehussein/AIA9k/index.html)

<sup>6</sup>[github.com/zalandoresearch/fashion-mnist](https://github.com/zalandoresearch/fashion-mnist)

- 179 3. Negating the intensities of the image to get white character with black background.  
 180 4. Computing the center of mass of the pixels.  
 181 5. Translating the image to put center of mass at the center of the  $28 \times 28$  grayscale image.

182 Some samples of the LPALIC dataset is visualized in Figure 1 for Latin characters and in Figure 2 for Arabic characters.

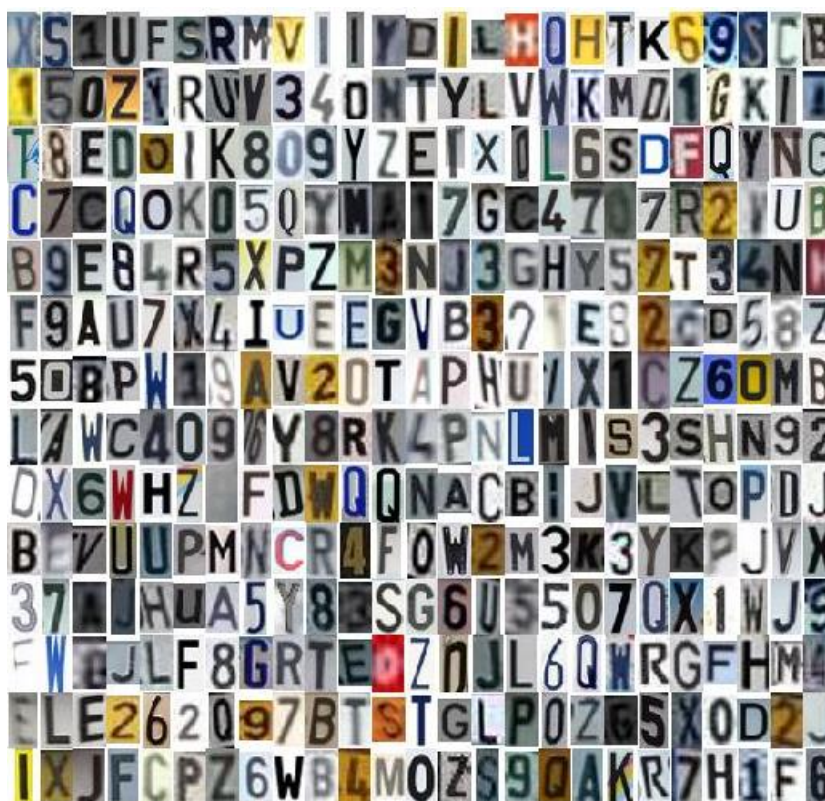


Figure 1. Samples of Latin characters in the LPALIC dataset.

183  
 184 Characters "0" and "O" are in the same class label so Latin characters have 35 (10 digits and 25  
 185 letters) class labels and Arabic characters have 27 (10 digits and 17 letters) class labels as LP as used in  
 KSA. Table 3 illustrates the total number of Arabic and Latin characters included in LPALIC dataset.

Table 3. LPALIC dataset number of cropped characters per country.

Country	TR	EU	USA	UAE	Others	KSA	
Used Characters	Latin	Latin	Latin	Latin & Arabic	Latin	Arabic	
Number of Characters	60000	32776	7384	3003	17613	50000	
Total Characters						120776	50000

186  
 187 The Latin characters were collected from 11 countries (LPs have different background and font  
 188 colors) while the Arabic characters were collected from only KSA (LPs have white background and black  
 189 character). Choosing those countries is related to the availability of those LPs for public use.

## 190 PROPOSED APPROACH

191 Stacked CNN architecture is simple, where each layer has a single input and a single output. For small size  
 192 images, the key efficient simple deep learning architecture was LeNet-5 (Lecun et al., 1998), it consists of



**Figure 2.** Samples of Arabic characters in the LPALIC dataset.

193 three convolutional, two pooling and one FC (Dense) layer. It was used and developed for the models  
 194 in (Cireşan et al., 2010) and in the main column of MCDNN in (Ciregan et al., 2012). Most of recent  
 195 architectures are sparse structure of CNN such as models in GoogleNet (Szegedy et al., 2015), ResNet  
 196 (He et al., 2016) and DensNet (Huang et al., 2017).

### 197 Proposed Architecture

198 The core of the proposed model is the convolution block which is a convolutional layer followed by  
 199 a batch normalization (BN) layer (Ioffe and Szegedy, 2015) and a non-linear activation ReLU layer  
 200 (Krizhevsky et al., 2012). This block is called standard convolutional layer in (Howard et al., 2017). The  
 201 proposed convolutional layers have kernels of size  $5 \times 5$  with a single stride. This kernel size showed  
 202 a good feature extraction capability in LeNet-5 (Lecun et al., 1998) for small images as it covers 3.2%  
 203 of the input image in every stride. However, the recent trends are to replace  $5 \times 5$  with 2 layers of  $3 \times 3$   
 204 kernels as in InceptionV3 (Szegedy et al., 2016). Figure 3 shows the architecture design of the proposed  
 model.

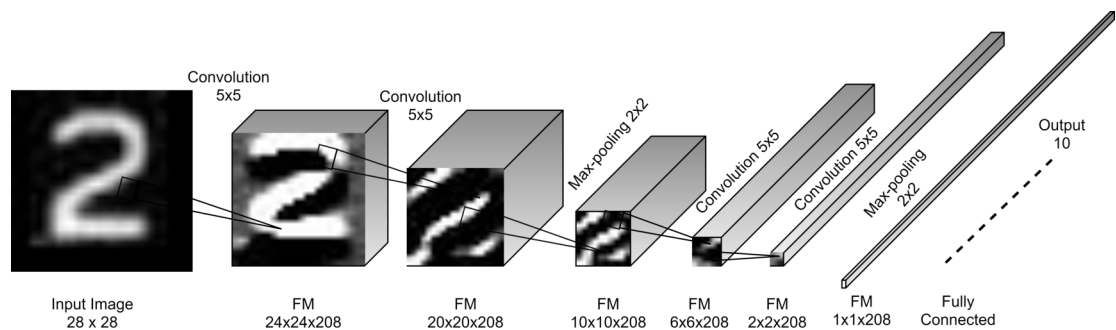


**Figure 3.** Proposed FDCNN model architecture.

205

206 BN layer was recently introduced by Ioffe and Szegedy (2015). It normalizes the input by subtracting  
 207 the mean of batch and dividing by the batch standard deviation then it scales and shifts the normalized  
 208 input by learnable scale and shift, it reduces covariance shift, reduces overfitting, enables higher learning

209 rates, regularizes the model and fulfills some of the same goals as Dropout layers. The first designers  
210 used BN layer in InceptionV3 are Szegedy et al. (2016).

For a mini-batch  $B = \{x_1, x_2, \dots, x_m\}$  of size  $m$ , the mean  $\mu_B$  and variance  $\sigma_B^2$  of  $B$  is computed and each input image in the mini-batch is normalized according to Equation (1).

$$\hat{x}_i = \frac{(x_i) - \mu_B}{\sqrt{\sigma_B^2 + \epsilon}} \quad (1)$$

Where  $\epsilon$  is a constant,  $\hat{x}_i$  is the  $i^{\text{th}}$  normalized image scaled by learnable scale parameter  $\gamma$  and shifted by learnable shift parameter  $\beta$  producing the  $i^{\text{th}}$  normalized output image  $y_i$  (Ioffe and Szegedy, 2015).

$$y_i = BN_{\gamma, \beta}(x_i) = \gamma \hat{x}_i + \beta \quad (2)$$

211 Motivated by LeNet-5 convolution kernel  $5 \times 5$ , BN used in InceptionV3 and ReLU in Alexnet, the proposed model convolution block is built as in Figure 4.

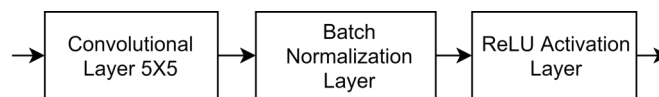


Figure 4. Proposed model convolution blocks.

212 The size of output feature map (FM) of each convolution block has lower size than the input feature map if no additional padding is applied. Equation (3) describes the relation between input and output FM sizes (Goodfellow et al., 2016).

$$W_y = \frac{W_x - W_k + 2P}{W_s} + 1 \quad (3)$$

213 Where  $W_y$  is the width of the output,  $W_x$  is the width of the input,  $W_k$  is the width of the kernel,  $W_s$  is  
214 the width of the stride kernel and  $P$  is the number of padding pixels. For the height  $H$ , Equation (3) can  
215 be used by replacing  $W$  with  $H$ . This reduction is called the shrinkage of convolution and it limits the  
216 number of convolutional layers that the network can include (Goodfellow et al., 2016). The feature map  
217 shrinks from borders to the center as convolutional layers as added. Eventually, feature maps drop to  
218  $1 \times 1 \times \text{channels}$  (single neuron per channel) at which no more convolutional layers can be added. This is  
219 the concept of full depth used for designing the proposed architecture, Figure 5 describes the full depth  
220 idea in FDCNN, where width and height shrink by 4 according to Equation (3). In Figure 5, each feature  
221 map is shrunk to a single value and this means that the features are convoluted into a single value resulting  
222 low number of parameters and high accuracy.

223 The proposed FDCNN model composed basically of two stacked convolutional stages and one FC  
224 layer for  $28 \times 28$  input images. Every stage has two convolution blocks and one max-pooling layer. It has  
225 a single input and a single output in all of its layers. Figure 3 shows the FDCNN architecture.

### 226 Parameter Selection

227 In the proposed architecture, there are some parameters have to be selected, these parameters are kernel  
228 sizes of convolution, pooling layers kernel sizes, the number of filters (channels) in convolution layers  
229 and strides. The kernel sizes are selected to be  $5 \times 5$  for convolutional layers and  $2 \times 2$  for pooling layers  
230 as described in architecture design in the previous Proposed Architecture section.

231 In literature, the trend for selecting the number of filters is to increase the number of filters as deep  
232 as the network goes (Krizhevsky et al., 2012; Szegedy et al., 2015; Simonyan and Zisserman, 2015; He  
233 et al., 2016). Generally, the first convolutional layers learn simple features while deeper layers learn more  
234 abstract features. Selecting optimal parameters is based on heuristics or grid searches (Bengio, 2012).  
235 The rule of thumb to design a network from scratch is to start with 8-64 filters per layer and double the  
236 number of filters after each pooling layer (Simonyan and Zisserman, 2015) or after each convolutional  
237 layer (He et al., 2016). Recently, a new method was proposed to select the number of filters (Garg et al.,  
238 2018), an optimization of network structure in terms of both the number of layers and the number of  
239 filters per layer was done using principal component analysis on trained network with a single shot of

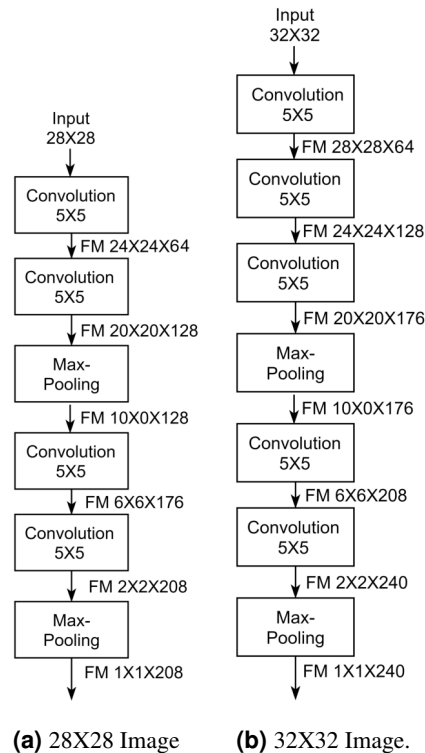


**Figure 5.** Full Depth concept of FDCNN.

240 analysis. A 9X reduction in the number of operations and up to 3X reduction in the number of parameters  
 241 with less than 1% drop in accuracy is achieved upon training on the same task. In context, a modeling  
 242 and optimization method (MAOM) was proposed in (Chou et al., 2019) to optimize CNN parameters by  
 243 integrating uniform experimental design (UED) and multiple regression (MR), but the rule of thumb for  
 244 doubling the number of filters was also applied.

245 One of the contributions of this research is to select the number of channels that achieves full depth.  
 246 Number of filters may also be called the number of kernels, number of layer channels or layers width.  
 247 The number of filters is selected to be as the same as the number of shrinking pixels in each layer from  
 bottom to the top. Table 4 shows the shrinkage of the proposed model. From the fact that the network

**Table 4.** Shrinkage process in  $28 \times 28$  architecture.

Layer	Shrinking Pixels	Width
Conv1	$28^2 - 24^2 = 208$	64
Conv2	$24^2 - 20^2 = 176$	128
Max-Pooling 1	—	128
Conv3	$10^2 - 6^2 = 64$	176
Conv4	$6^2 - 2^2 = 32$	208
Max-Pooling 2	—	208

248 goes more deeper the following selection is made:  
 249

- 250 • The width of  $4^{th}$  convolutional layer is 208 (the  $1^{st}$  layer shrinkage).
- 251 • The width of  $3^{rd}$  is 176 (the the  $2^{nd}$  layer shrinkage).
- 252 • The max-pooling will make a loss of half in FM dimensions so the next layers shrinkage pixels will  
 253 be doubled.
- 254 • The width of  $2^{nd}$  is 128 (the double of the  $3^{rd}$  layer shrinkage).

- 255 • The width of 1<sup>nd</sup> is 64 (the double of the 4<sup>th</sup> layer shrinkage).

256 The same parameter selection method can be applied to  $32 \times 32$  input architecture as described in  
 257 Table 5 to reach full depth features (single value feature) as shown in Figure 5b.

**Table 5.** Shrinkage process in  $32 \times 32$  architecture.

Layer	Shrinking Pixels	Width
Conv1	$32^2 - 28^2 = 240$	64
Conv2	$28^2 - 24^2 = 208$	128
Conv3	$24^2 - 20^2 = 176$	176
Max-Pooling 1	---	176
Conv4	$10^2 - 6^2 = 64$	208
Conv5	$6^2 - 2^2 = 32$	240
Max-Pooling 2	---	240

258 Table 6 shows the number of learnable parameters and feature memory usage for the proposed model.  
 259 Memory usage is multiplied by 4 as each pixel is stored as 4-byte single float number. For  $32 \times 32$  input  
 260 images just another convolutional block can be added before the first convolution block in FDCNN and  
 261 the width of last convolutional layer will be  $32^2 - 28^2 = 240$  to get full depth of shrinkage. This layer of  
 262 course affects the total number of model parameters and FM memory usage to be 2.94M and 2.51MB  
 263 respectively.

**Table 6.** Proposed model's memory usage and learnable parameters.

Layer	Features Memory		Learnable Parameters	
Input	$28 \times 28 \times 1$	3136	0	0
Conv1	$24 \times 24 \times 64$	147456	$(5 \times 5) \times 64 + 64 =$	1664
BN+ReLU	$24 \times 24 \times 64 \times 2$	294912	$4 \times 64 =$	256
Conv2	$20 \times 20 \times 128$	204800	$5 \times 5 \times 64 \times 128 + 128 =$	204928
BN+ReLU	$20 \times 20 \times 128 \times 2$	409600	$4 \times 128 =$	512
Max-pooling1	$10 \times 10 \times 128$	51200	0	0
Conv3	$6 \times 6 \times 176$	25344	$5 \times 5 \times 128 \times 176 + 176 =$	563376
BN+ReLU	$6 \times 6 \times 176 \times 2$	50688	$4 \times 176 =$	704
Conv4	$2 \times 2 \times 208$	3328	$5 \times 5 \times 176 \times 208 + 208 =$	915408
BN+ReLU	$2 \times 2 \times 208 \times 2$	6656	$4 \times 208 =$	832
Max-pooling2	$1 \times 1 \times 208$	832	0	0
FC	$1 \times 1 \times 10$	40	$208 \times 10 + 10 =$	2090
	Total Memory	1197992 Bytes	Total Parameters	1689770

264 In general, DNNs give weights for all input features (neurons) to produce the output neurons, but this  
 265 needs a huge number of parameters. Instead, CNNs convolve the adjacent neurons by the convolution  
 266 kernel size to produce the output neurons. In the literature, the state-of-the-art architectures had high  
 267 number of learnable parameters at the last FC layers. For example, VGG16 has totally 136M parameters,  
 268 and after the last pooling layer the first FC layer has 102M parameters, which means more than 75%  
 269 of the architecture parameters (just in one layer). AlexNet has totally 62M parameters, and the first FC  
 270 layer has 37.75M parameters, which means more than 60% of the architecture parameters. In (Hirata and  
 271 Takahashi, 2020), the proposed architecture has 28.68M parameters, and the first FC layer has 3.68M  
 272 parameters after majority voting from ten divisions. But, by using the full depth concept to reduce FM to  
 273  $1 \times 1$  size after the last pooling layer, FDCNN has just 2090 parameters from totally 1.6M parameters as  
 274 seen in Table 6. The full depth concept of reducing the feature maps size to one neuron has decreased the  
 275 total number of learnable parameters which make FDCNN simple and fast.

## 276 Training Process

277 Deep learning training algorithms were well explained in (Goodfellow et al., 2016). The proposed model  
 278 is trained using stochastic gradient descent with momentum (SGDM) with custom parameters chosen  
 279 after many trails, initial learning rate (LR) of 0.025, mini-batch size equals to the number of training  
 280 instances divided by number of batches needed to complete one epoch, LR drop factor by half every 2  
 281 epochs, 10 epochs, 0.95 momentum and the training set is shuffled every epoch. However, those training  
 282 parameters are not used for all datasets since the number of images is not constant in all of them.

283 After getting the first results, The model parameters are tuned by training again on ADAM with larger  
 284 mini-batch size and very small LR started by  $1 \times 10^{-5}$ , then multiplying the batch size by 2 and LR by  
 285 1/2 every 10 epochs as long as the test error has improvement.

## 286 EXPERIMENTAL RESULTS AND DISCUSSION

287 All of training and testing are made on MATLAB2018 platform with GeForce 1060 (6GB shared memory  
 288 GPU). The main goal of this research is to design a CNN to recognize multi-language characters of  
 289 license plates but to generalize and verify the designed architecture several tests on handwritten character  
 290 recognition benchmarks are done (verification process). The proposed approach showed very promising  
 results. Table 7 summarizes the results obtained on MNIST dataset.

**Table 7.** Test results of FDCNN on MNIST.

Architecture	Type	Number of Layers	Error
Cireşan et al. (2010)	stacked	15	0.35%
Ciresan et al. (2011)	sparse	35	0.27%
Ciregan et al. (2012)	sparse	245	0.23%
Moradi et al. (2019)	sparse	70	0.28%
Kowsari et al. (2018)	sparse	—	0.18%
Assiri (2019)	stacked	15	0.17%
Hirata and Takahashi (2020)	sparse	28	0.16%
Byerly et al. (2020)	sparse	21	0.16%
Proposed	stacked	<b>12</b>	0.28%

291  
 292 It is clear that stacked CNN has not outperformed the error of 0.35% in the literature for MNIST but  
 293 the approach used in (Assiri, 2019) obtained 0.17%. The proposed FDCNN performance approximately  
 294 reached close to the performance of five committees CNN of (Ciresan et al., 2011). FDCNN do as the  
 295 same performance as (Moradi et al., 2019) which it is a sparse design that uses Residual blocks and  
 296 Inception blocks as described in the literature. However, the architecture in (Assiri, 2019) has 15 layers  
 297 with 13.12M parameters while FDCNN has 12 layers with 1.69M parameters which means that FDCNN is  
 298 simpler and 7 times faster (in terms of number of the parameters 13.12/1.69). The results in (Assiri, 2019)  
 299 were obtained utilizing data augmentations (not used in FDCNN training), different training processes  
 300 (FDCNN training process is simpler as described in the previous section) and Dropout layers before and  
 301 after each pooling layer with different settings, but FDCNN has no Dropout layer and showed good results  
 302 on MNIST.

303 On the other hand, the proposed approach is tested on MADbase, AHCD and AI9IK datasets for  
 304 Arabic character recognition benchmarks to verify FDCNN and to generalize using it in Arabic ALPR  
 305 systems. Table 8 describes the classification error regarding the stat-of-the-art on such datasets. The same  
 306 logic of size-sensitive feature proposed in (Abdleazeem and El-Sherif, 2008) is used to solve the problem  
 307 of Arabic zero character by half size reduction for Arabic zero character images (in MADbase dataset)  
 308 since it has a smaller size than other characters.

309 As seen in Table 8, for MADbase dataset, most of the tested approaches were based on VGG  
 310 architecture. Alphanumeric VGG (Mudhsh and Almodfer, 2017) reported a validation error of 0.34%  
 311 that did not hold on the test set while FDCNN obtained 0.15% validation error and 0.34% test error. The  
 312 proposed approach outperformed Arabic character recognition benchmarks state-of-the-arts for both digits  
 313 and letters used in Arabic language with less number of layers and learnable parameters. It has succeed  
 314 this verification process on these datasets too.

**Table 8.** Arabic character recognition benchmarks state-of-the-art and proposed approach test errors.

Dataset	Architecture	Type	Layers	Parameters	Error
MADbase 28 × 28	RBF SVM Abdleazeem and El-Sherif (2008)	linear	—	—	0.52%
	LeNet5 El-Sawy et al. (2017)	stacked	7	51K	12%
	Alphanumeric VGG Mudhsh and Almodfer (2017)	stacked	17	2.1M	0.34% validation
	VGG12_REGU Sousa (2018)	Average of 4 stacked CNN	66	18.56M	0.48%
	proposed	stacked	12	1.69M	<b>0.34%</b>
AHCD 32 × 32	CNN El-Sawy et al. (2017)	stacked	7	1.8M	5.1%
	CNN Younis (2017)	stacked	6	200K	2.4%
	VGG12_REGU Sousa (2018)	Average of 4 stacked CNN	66	18.56M	1.58%
	CNN Najadat et al. (2019)	stacked	10	Not mentioned	2.8%
	proposed	stacked	13	2.94M	<b>1.39%</b>
AI9IK 32 × 32	RBF SVM Torki et al. (2014)	linear	—	—	5.72%
	CNN Younis (2017)	stacked	6	200K	5.2%
	proposed	stacked	13	2.94M	<b>3.27%</b>

315 In Table 8, input layer is included in the determination of the number layers (Lecun et al., 1998) for  
 316 all architectures and ReLU layer is not considered as a layer but BN is considered as a layer. Sousa (2018)  
 317 considered convolution, pooling and FC layers when the number of layers was declared but four trained  
 318 CNNs were used with softmax averaging, this is why the number of layers and learnable parameters  
 319 are high. Najadat et al. (2019) did not declare the most of network parameters like kernel size in every  
 320 convolution layer and they changed many parameters to enhance the model. In (Younis, 2017), 28 × 28  
 321 input images were used and no pooling layers were included.

322 On the other hand, and in the same verification process, the proposed approach is also tested on  
 323 FashionMNIST benchmark to generalize using it over grayscale tiny images. As shown in Table 9, the  
 324 proposed approach outperformed the stacked CNN architectures and reached near DENSER network  
 325 in (Assunção et al., 2018) and EnsNet in (Hirata and Takahashi, 2020) with less layers and parameters  
 326 but with a good performance. It can be said that FDCNN has a very good verification performance  
 327 on FashionMNIST dataset. FDCNN outperformed (Byerly et al., 2020) results on Fashion-MNIST  
 benchmark while (Byerly et al., 2020) outperformed FDCNN on MNIST.

**Table 9.** Test results of FDCNN on FashionMNIST.

Architecture	Type	Layers	Parameters	Error
SVM (Xiao et al., 2017)	linear	—	—	10.3%
DENSER (Assunção et al., 2018)	sparse	—	—	4.7%
WRN (Zhong et al., 2017)	sparse	28	36.5M	3.65%
VGG16 (Zeng et al., 2018)	sparse	16	138M	2.34%
CNN (Chou et al., 2019)	stacked	16	0.44M	8.32%
BRCNN (Byerly et al., 2020)	sparse	16	1.51M	6.34%
EnsNet (Hirata and Takahashi, 2020)	sparse	28	28.67M	4.7%
Proposed	stacked	<b>12</b>	<b>1.69M</b>	<b>5.00%</b>

328

329 All of the previous datasets were divided into training and test sets by their authors where the instances  
 330 in the test set were collected from a different source (different writers for CR and different photographers  
 331 for fashion) from the training set's source. The performance evaluation is done based on CNN type  
 332 (stacked is simpler than spars), number of layers, number of learnable parameters and recognition error.

333 Furthermore, FDCNN is tested also on Arabic LP characters from KSA. However, Khaled et al. (2010)  
 334 used his dataset for both training and testing, FDCNN could classify the whole dataset (as a test set)  
 335 of (Khaled et al., 2010) with error of 0.46% whereas the training was done on characters collected and  
 336 cropped manually from public KSA LP images. It outperformed the recognition error results of 1.78% in  
 337 (Khaled et al., 2010). FDCNN has successfully verified on KSA Arabic LP characters dataset.

338 In this research and for more verification, FDCNN performance is also tested on both common  
 339 publicly available LP benchmark characters and the new LPALIC dataset. Table 10 shows the promising  
 340 results on LP benchmarks. FDCNN outperformed the state-of-the-art results on common LP datasets for  
 341 isolated character recognition problem. Zemris, UCSD, Snapshots and ReID datasets were not used in  
 342 the training process but the proposed FDCNN was tested on each of them as a test set to ensure that the  
 343 model was fitted to character features, not to a dataset itself. For UFPR dataset, FDCNN was tested two  
 344 times on UFPR test set, training on only the training set of UFPR and training on both UFPR and LPALIC  
 345 characters. It is clear that FDCNN has efficiently verified on common LP benchmarks.

**Table 10.** Recognition error of proposed architecture on LP benchmarks datasets.

Architecture	Dataset	Layers	Parameters	Error
SVM (Panahi and Gholampour, 2017)	Zemris	—	—	3%
LCR-Alexnet (Meng et al., 2018)		12	>2.33M	2.7%
Proposed		12	1.69M	<b>0.979%</b>
OCR (Dlagnekov, 2005)	UCSD	—	—	10.5%
Proposed		12	1.69M	<b>1.51%</b>
MLP (Martinsky, 2007)	Snapshots	—	—	15%
Proposed		12	1.69M	<b>0.42%</b>
CNN (Špaňhel et al., 2017)	ReID	12	17M	3.5%
DenseNet169 (Zhu et al., 2019)		169	>15.3M	6.35%
Proposed		12	1.69M	<b>1.09%</b>
CNN (Laroca et al., 2018)	UFPR	26	43.1M	35.1%
Proposed trained just on UFPR		12	1.69M	4.29%
Proposed trained on LPALIC		12	1.69M	<b>2.03%</b>
Line Processing Algorithm (Khaled et al., 2010)	KSA	—	—	1.78%
Proposed		12	1.69M	<b>0.46%</b>
FDCNN	LPALIC	12	1.69M	0.97%

346 For more analysis, another test is made on the introduced LPALIC dataset to analyze the recognition  
 347 error on characters per country. Table 11 describes the results. As seen in Table 11, the highest error is in  
 348 classifying USA LP characters because it has more colors, drawings and shapes other than characters  
 349 and also there is a small number of instances in the characters dataset. However, a very high recognition  
 350 accuracy is achieved on Turkey and EU since they have the same standard and style for LPs. In Turkey, 10  
 351 digits and 23 letter is used since letters like Q, W and X are not valid in Turkish language. Additionally,  
 352 FDCNN could classify Arabic LP characters with very low error. UAE characters set has a small number  
 353 of cropped characters that is why it is tested just by FDCNN trained on other countries character sets.

354 To make robust tests, the characters were split manually and randomly as seen in Table 11. In  
 355 manual split, the most difficult characters (difficult at manual labelling the character images in the dataset  
 356 preparing stage) were put in the test set and the others in the training set while in random split 80% were  
 357 split for training and the rest of them for testing. As described in Table 3, the number of characters per  
 358 country is not equal, which resulted various recognition accuracies in Table 11. Since the number of  
 359 UAE characters is not large enough to train FDCNN, Latin characters from other countries were used for  
 360 training but the test was done only on UAE test set. FDCNN could learn features that give good average  
 361 accuracy.

**Table 11.** Test recognition error per country characters with different training instances.

Characters Set	Number of Instances Train / Test	Manual Split	Trained on Other Countries	Random 80/20% Split Average Error	Random 70/10/20% Split Average Error
TR	48748 / 11755	2.67%	1.82%	0.97%	0.99%
EU	23299 / 9477	2.30%	1.07%	1.03%	0.80%
USA	5960 / 1424	10.88%	3.51%	1.96%	1.79%
UAE	1279 / 1724	—	1.51%	0.9%	1.08%
All Latin Characters	96899 / 24380	2.08%	—	0.97%	1.06%
KSA	46981 / 3018	0.43%	—	0.26%	0.30%

362 In the manual split in Table 11, the country's characters training and testing sets were used to train  
 363 and test FDCNN. In trained on other countries, the FDCNN was trained on both the country's characters  
 364 training set and other countries characters but tested only on that country's test set. In the random 80/20  
 365 split, the country's characters were split randomly into training and testing sets, and FDCNN was trained  
 366 on both the split country's characters training set and other countries characters but tested only on that  
 367 split country's test set, a lot of random split tests were done and the average errors were reported in the  
 368 table.

369 Furthermore, in Table 11, validation sets were also used to guarantee in a sufficiently clear way that  
 370 the results were not optimized specifically for those test sets. 70% of the dataset is randomly split for  
 371 training, 10% for validation and 20% for testing. The training hyperparameters were optimized on a  
 372 validation set, and the best parameters for the validation set were then be used to calculate the error on  
 373 the test set. Those different test analyses were done to validate and evaluate the results and reduce the  
 374 overfitting problem. In fact, the Latin characters in LPALIC have various background and foreground  
 375 colors which make the classification more challenging than Arabic characters set, but FDCNN shows a  
 376 promising recognition results on both and also on handwritten characters as well.

## 377 CONCLUSION

378 This research focused on deep learning technique of CNNs to recognize multi-language LP characters  
 379 for both Latin and Arabic characters used in vehicle LPs. A new approach is proposed, analyzed and  
 380 tested on Latin and Arabic CR benchmarks for both LP and handwritten characters recognition. The  
 381 proposed approach consists of proposing FDCNN architecture, FDCNN parameter selection and training  
 382 process. The proposed full depth and width selection ideas are very efficient in extracting features from  
 383 tiny grayscale images. The complexity of FDCNN is also analyzed in terms of number of learnable  
 384 parameters and feature maps memory usage. The full depth concept of reducing the feature maps size to  
 385 one neuron has decreased the total number of learnable parameters while achieving very good results.  
 386 Implementation of FDCNN approach is simple and can be used in real time applications worked on  
 387 small devices like mobiles, tablets and some embedded systems. Very promising results were achieved  
 388 on some common benchmarks like MNIST, FashionMNIST, MADbase, AIA9K, AHCD, Zemris, ReId,  
 389 UFPR and the newly introduced LPALIC dataset. FDCNN performance is verified and compared to the  
 390 state-of-the-art results in the literature. A new real LPs cropped characters dataset is also introduced. It is  
 391 the largest dataset for LP characters in Turkey and KSA. More tests can be done on FDCNN for future  
 392 work to be the core of CNN processor. Also, more experiments can be conducted to hybrid FDCNN with  
 393 some common blocks like residual and inception blocks. Additionally, the proposed full depth approach  
 394 may be applied to other stacked CNNs like Alexnet and VGG networks.

## 395 REFERENCES

- 396 Abdleazeem, S. and El-Sherif, E. (2008). Arabic handwritten digit recognition. *International Journal of*  
 397 *Document Analysis and Recognition (IJ DAR)*, 11(3):127–141.  
 398 Asif, M. R., Chun, Q., Hussain, S., Fareed, M. S., and Khan, S. (2017). Multinational vehicle license  
 399 plate detection in complex backgrounds. *Journal of Visual Communication and Image Representation*,  
 400 46:176 – 186.

- 401 Asif, M. R., Qi, C., Wang, T., Fareed, M. S., and Raza, S. A. (2019). License plate detection for  
402 multi-national vehicles: An illumination invariant approach in multi-lane environment. *Computers &*  
403 *Electrical Engineering*, 78:132 – 147.
- 404 Assiri, Y. S. (2019). Stochastic optimization of plain convolutional neural networks with simple methods.  
405 In *15th International Conference on Machine Learning and Data Mining, MLDM*, volume 2, pages  
406 833–844. ibai-publishing.
- 407 Assunção, F., Lourenço, N., Machado, P., and Ribeiro, B. (2018). DENSER: deep evolutionary network  
408 structured representation. *CoRR*, abs/1801.01563.
- 409 Bengio, Y. (2012). *Practical Recommendations for Gradient-Based Training of Deep Architectures*, pages  
410 437–478. Springer Berlin Heidelberg, Berlin, Heidelberg.
- 411 Bulan, O., Kozitsky, V., and Burry, A. (2015). Towards annotation free license plate recognition. In *IEEE*  
412 *18th International Conference on Intelligent Transportation Systems*, pages 1495–1499.
- 413 Bulan, O., Kozitsky, V., Ramesh, P., and Shreve, M. (2017). Segmentation- and annotation-free license  
414 plate recognition with deep localization and failure identification. *IEEE Transactions on Intelligent*  
415 *Transportation Systems*, 18(9):2351–2363.
- 416 Byerly, A., Kalganova, T., and Dear, I. (2020). A branching and merging convolutional network with  
417 homogeneous filter capsules. *ArXiv*, abs/2001.09136.
- 418 Chou, F., Tsai, Y., Chen, Y., Tsai, J., and Kuo, C. (2019). Optimizing parameters of multi-layer  
419 convolutional neural network by modeling and optimization method. *IEEE Access*, 7:68316–68330.
- 420 Cireşan, D. C., Meier, U., Gambardella, L. M., and Schmidhuber, J. (2010). Deep, big, simple neural nets  
421 for handwritten digit recognition. *Neural Computation*, 22(12):3207–3220.
- 422 Ciregan, D., Meier, U., and Schmidhuber, J. (2012). Multi-column deep neural networks for image  
423 classification. In *IEEE Conference on Computer Vision and Pattern Recognition*, pages 3642–3649.
- 424 Ciresan, D. C., Meier, U., Gambardella, L. M., and Schmidhuber, J. (2011). Convolutional neural network  
425 committees for handwritten character classification. In *International Conference on Document Analysis*  
426 *and Recognition*, pages 1135–1139.
- 427 Comelli, P., Ferragina, P., Granieri, M. N., and Stabile, F. (1995). Optical recognition of motor vehicle  
428 license plates. *IEEE Transactions on Vehicular Technology*, 44(4):790–799.
- 429 Dlagnekov, L. (2005). Video-based car surveillance: License plate, make, and model recognition. Master’s  
430 thesis, University of California, San Diego.
- 431 Dorbe, N., Jaundalders, A., Kadikis, R., and Nesenbergs, K. (2018). Fcn and lstm based computer vision  
432 system for recognition of vehicle type, license plate number, and registration country. *Automatic*  
433 *Control and Computer Sciences*, 52(2):146–154.
- 434 Du, S., Ibrahim, M., Shehata, M., and Badawy, W. (2013). Automatic license plate recognition (alpr): A  
435 state-of-the-art review. *IEEE Transactions on Circuits and Systems for Video Technology*, 23(2):311–  
436 325.
- 437 El-Sawy, A., EL-Bakry, H., and Loey, M. (2017). Cnn for handwritten arabic digits recognition based on  
438 lenet-5. In Hassanien, A. E., Shaalan, K., Gaber, T., Azar, A. T., and Tolba, M. F., editors, *International*  
439 *Conference on Advanced Intelligent Systems and Informatics*, pages 566–575. Springer International  
440 Publishing.
- 441 El-Sawy, A., Loey, M., and EL-Bakry, H. (2017). Arabic handwritten characters recognition using  
442 convolutional neural network. *WSEAS Transactions on Computer Research*, 5:11–19.
- 443 El-Sherif, E. A. and Abdelazeem, S. (2007). A two-stage system for arabic handwritten digit recognition  
444 tested on a new large database. In *Artificial Intelligence and Pattern Recognition*.
- 445 Eltay, M., Zidouri, A., and Ahmad, I. (2020). Exploring deep learning approaches to recognize handwritten  
446 arabic texts. *IEEE Access*, 8:89882–89898.
- 447 Fernández, F., Negri, P., Mejail, M., and Jacobo, J. (2011). A multi-style license plate recognition system  
448 based on tree of shapes for character segmentation. In San Martin, C. and Kim, S.-W., editors, *Progress*  
449 *in Pattern Recognition, Image Analysis, Computer Vision, and Applications*, pages 443–450. Springer  
450 Berlin Heidelberg.
- 451 Garg, I., Panda, P., and Roy, K. (2018). A low effort approach to structured CNN design using PCA.  
452 *CoRR*, abs/1812.06224.
- 453 Gonçalves, G. R., Menotti, D., and Schwartz, W. R. (2016). License plate recognition based on temporal  
454 redundancy. In *IEEE International Conference on Intelligent Transportation Systems (ITSC)*, pages  
455 2577–2582.

- 456 Goodfellow, I., Bengio, Y., and Courville, A. (2016). *Deep Learning*. MIT Press.
- 457 Guha, R., Das, N., Kundu, M., Nasipuri, M., and Santosh, K. C. (2020). Devnet: An efficient cnn archi-  
458 tecture for handwritten devanagari character recognition. *International Journal of Pattern Recognition*  
459 *and Artificial Intelligence*, 34(12):2052009.
- 460 He, K., Zhang, X., Ren, S., and Sun, J. (2016). Deep residual learning for image recognition. In *IEEE*  
461 *Conference on Computer Vision and Pattern Recognition (CVPR)*, pages 770–778.
- 462 Henry, C., Ahn, S. Y., and Lee, S. (2020). Multinational license plate recognition using generalized  
463 character sequence detection. *IEEE Access*, 8:35185–35199.
- 464 Hirata, D. and Takahashi, N. (2020). Ensemble learning in cnn augmented with fully connected subnet-  
465 works. *ArXiv*, abs/2003.08562.
- 466 Howard, A. G., Zhu, M., Chen, B., Kalenichenko, D., Wang, W., Weyand, T., Andreetto, M., and Adam,  
467 H. (2017). Mobilenets: Efficient convolutional neural networks for mobile vision applications. *CoRR*,  
468 abs/1704.04861.
- 469 Huang, G., Liu, Z., v. d. Maaten, L., and Weinberger, K. Q. (2017). Densely connected convolutional  
470 networks. In *IEEE Conference on Computer Vision and Pattern Recognition (CVPR)*, pages 2261–2269.
- 471 Iandola, F. N., Moskewicz, M. W., Ashraf, K., Han, S., Dally, W. J., and Keutzer, K. (2016). Squeezenet:  
472 Alexnet-level accuracy with 50x fewer parameters and 1mb model size. *CoRR*, abs/1602.07360.
- 473 Ioffe, S. and Szegedy, C. (2015). Batch normalization: Accelerating deep network training by reduc-  
474 ing internal covariate shift. In *Proceedings of the 32Nd International Conference on International*  
475 *Conference on Machine Learning*, volume 37 of *ICML'15*, pages 448–456. JMLR.org.
- 476 Khaled, M. A., Rached, N. Z., and Hasan, R. O. (2010). Pixel density: Recognizing characters in saudi  
477 license plates. In *10th International Conference on Intelligent Systems Design and Applications*, pages  
478 308–313.
- 479 Kowsari, K., Heidarysafa, M., Brown, D. E., Meimandi, K. J., and Barnes, L. E. (2018). Rmdl: Random  
480 multimodel deep learning for classification. In *Proceedings of the 2nd International Conference on*  
481 *Information System and Data Mining, ICISDM '18*, page 19–28, New York, NY, USA. Association for  
482 Computing Machinery.
- 483 Kraupner, K. (2003). Using multilayer perceptron to recognize numeric-alphanumeric characters on  
484 license plates. Bsc. eng. thesis, University of Zagreb, Croatia.
- 485 Krizhevsky, A., Sutskever, I., and Hinton, G. E. (2012). Imagenet classification with deep convolutional  
486 neural networks. In Pereira, F., Burges, C. J. C., Bottou, L., and Weinberger, K. Q., editors, *Advances*  
487 *in Neural Information Processing Systems 25*, pages 1097–1105. Curran Associates, Inc.
- 488 Laroca, R., Severo, E., Zanlorensi, L. A., Oliveira, L. S., Gonçalves, G. R., Schwartz, W. R., and Menotti,  
489 D. (2018). A robust real-time automatic license plate recognition based on the YOLO detector. In  
490 *International Joint Conference on Neural Networks (IJCNN)*, pages 1–10.
- 491 Le, N. Q. K. and Nguyen, V.-N. (2019). Snare-cnn: a 2d convolutional neural network architecture to  
492 identify snare proteins from high-throughput sequencing data. *PeerJ Computer Science*, 5:e177.
- 493 Lecun, Y., Bottou, L., Bengio, Y., and Haffner, P. (1998). Gradient-based learning applied to document  
494 recognition. *Proceedings of the IEEE*, 86(11):2278–2324.
- 495 Li, H., Wang, P., and Shen, C. (2019). Toward end-to-end car license plate detection and recognition with  
496 deep neural networks. *IEEE Transactions on Intelligent Transportation Systems*, 20(3):1126–1136.
- 497 Martinsky, O. (2007). Algorithmic and mathematical principles of automatic number plate recognition  
498 systems. B.sc. eng. thesis, Brno University of Technology, Croatia.
- 499 Meng, A., Yang, W., Xu, Z., Huang, H., Huang, L., and Ying, C. (2018). A robust and efficient method  
500 for license plate recognition. In *24th International Conference on Pattern Recognition (ICPR)*, pages  
501 1713–1718.
- 502 Moradi, R., Berangi, R., and Minaei, B. (2019). Orthomaps: an efficient convolutional neural network  
503 with orthogonal feature maps for tiny image classification. *IET Image Processing*, 13(12):2067–2076.
- 504 Mudhsh, M. and Almodfer, R. (2017). Arabic handwritten alphanumeric character recognition using very  
505 deep neural network. *Information*, 8(3):105.
- 506 Najadat, H. M., Alshboul, A. A., and Alabed, A. F. (2019). Arabic handwritten characters recognition  
507 using convolutional neural network. In *IEEE 10th International Conference on Information and*  
508 *Communication Systems (ICICS)*, pages 147–151.
- 509 Netzer, Y., Wang, T., Coates, A., Bissacco, A., Wu, B., and Ng, A. Y. (2011). Reading digits in natural  
510 images with unsupervised feature learning. In *NIPS Workshop on Deep Learning and Unsupervised*

- 511 *Feature Learning 2011.*
- 512 Panahi, R. and Gholampour, I. (2017). Accurate detection and recognition of dirty vehicle plate numbers  
513 for high-speed applications. *IEEE Transactions on Intelligent Transportation Systems*, 18(4):767–779.
- 514 Park, S., Yoon, H., and Park, S. (2019). Multi-style license plate recognition system using k-nearest  
515 neighbors. *KSII Transactions on Internet and Information Systems*, 13(5):2509–2528.
- 516 Salemedeb, M. and Erturk, S. (2020). Multi-national and multi-language license plate detection using  
517 convolutional neural networks. *Engineering, Technology Applied Science Research*, 10(4):5979–5985.
- 518 Selmi, Z., Halima, M. B., Pal, U., and Alimi, M. A. (2020). Delp-dar system for license plate detection  
519 and recognition. *Pattern Recognition Letters*, 129:213 – 223.
- 520 Shyang-Lih Chang, Li-Shien Chen, Yun-Chung Chung, and Sei-Wan Chen (2004). Automatic license  
521 plate recognition. *IEEE Transactions on Intelligent Transportation Systems*, 5(1):42–53.
- 522 Simonyan, K. and Zisserman, A. (2015). Very deep convolutional networks for large-scale image  
523 recognition. In *International Conference on Learning Representations*.
- 524 Sousa, I. P. D. (2018). Convolutional ensembles for arabic handwritten character and digit recognition.  
525 *PeerJ Computer Science*, 4:e167V.
- 526 Špaňhel, J., Sochor, J., Juránek, R., Herout, A., Maršík, L., and Zemčík, P. (2017). Holistic recognition of  
527 low quality license plates by cnn using track annotated data. In *14th IEEE International Conference on*  
528 *Advanced Video and Signal Based Surveillance (AVSS)*, pages 1–6. IEEE.
- 529 Szegedy, C., Vanhoucke, V., Ioffe, S., Shlens, J., and Wojna, Z. (2016). Rethinking the inception  
530 architecture for computer vision. In *The IEEE Conference on Computer Vision and Pattern Recognition*  
531 *(CVPR)*.
- 532 Szegedy, C., Wei Liu, Yangqing Jia, Sermanet, P., Reed, S., Anguelov, D., Erhan, D., Vanhoucke, V., and  
533 Rabinovich, A. (2015). Going deeper with convolutions. In *IEEE Conference on Computer Vision and*  
534 *Pattern Recognition (CVPR)*, pages 1–9.
- 535 Torki, M., Hussein, M. E., Elsallamy, A., Fayyaz, M., and Yaser, S. (2014). Window-based descriptors for  
536 arabic handwritten alphabet recognition: A comparative study on a novel dataset. *ArXiv*, abs/1411.3519.
- 537 Xiao, H., Rasul, K., and Vollgraf, R. (2017). Fashion-mnist: a novel image dataset for benchmarking  
538 machine learning algorithms. *CoRR*, abs/1708.07747.
- 539 Xie, L., Ahmad, T., Jin, L., Liu, Y., and Zhang, S. (2018). A new cnn-based method for multi-directional  
540 car license plate detection. *IEEE Transactions on Intelligent Transportation Systems*, 19(2):507–517.
- 541 Xu, Z., Yang, W., Meng, A., Lu, N., and Huang, H. (2018). Towards end-to-end license plate detection  
542 and recognition: A large dataset and baseline. In *Proceedings of the European Conference on Computer*  
543 *Vision (ECCV)*, pages 255–271.
- 544 Younis, K. (2017). Arabic handwritten character recognition based on deep convolutional neural networks.  
545 *Jordanian Journal OF Computers and Information Technology (JJCIT)*, 3(3):186–200.
- 546 Yépez, J., Castro-Zunti, R. D., and Ko, S. (2019). Deep learning-based embedded license plate localisation  
547 system. *IET Intelligent Transport Systems*, 13(10):1569–1578.
- 548 Zagoruyko, S. and Komodakis, N. (2016). Wide residual networks. In *Proceedings of the British Machine*  
549 *Vision Conference (BMVC)*, pages 87.1–87.12. BMVA Press.
- 550 Zeng, S., Zhang, B., Zhang, Y., and Gou, J. (2018). Collaboratively weighting deep and classic represen-  
551 tation via  $l_2$  regularization for image classification. In *Proceedings of The 10th Asian Conference on*  
552 *Machine Learning*, volume 95, pages 502–517.
- 553 Zhong, Z., Zheng, L., Kang, G., Li, S., and Yang, Y. (2017). Random erasing data augmentation. *CoRR*,  
554 abs/1708.04896.
- 555 Zhu, L., Wang, S., Li, C., and Yang, Z. (2019). License plate recognition in urban road based on vehicle  
556 tracking and result integration. *Journal of Intelligent Systems*, 0(0).